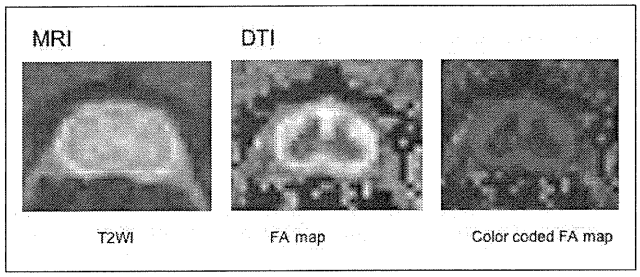

Fig.3 MRI and DTI of the normal spinal cord of a common marmoset

T2-weighted image (T2WI) and DTI (anisotropy map and colored anisotropy map) of the common marmoset spinal cord (cross-section). On the anisotropy map, white matter fibers, which have high anisotropy, are depicted as high signal areas. On the colored anisotropy map, different colors are assigned to different axes. White matter fibers are blue. The image shows the white matter to be composed of longitudinally arranged axonal fibers. (Reproduced from Reference 26)

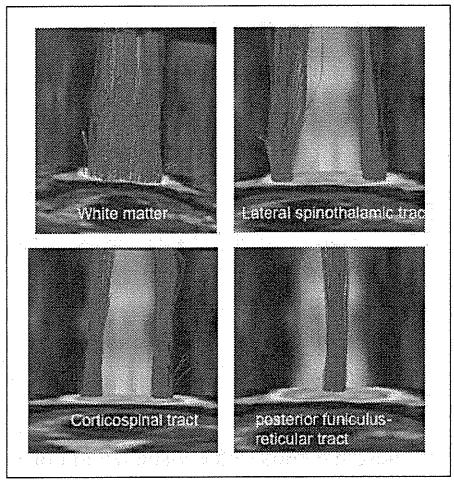

Fig.5 DTT of the normal spinal cord of a common marmoset (live model)

DTT clearly depicting fibers of the entire white matter were obtained by setting the regions of interest within the white matter of the cervical segment of the common marmoset spinal cord. By changing the regions of interest, it is possible to selectively depict by DTT, not only the corticospinal tract, but also the afferent fibers (lateral spinothalamic tract, posterior funiculus-reticular tract, etc.). (Reproduced from Reference 26)

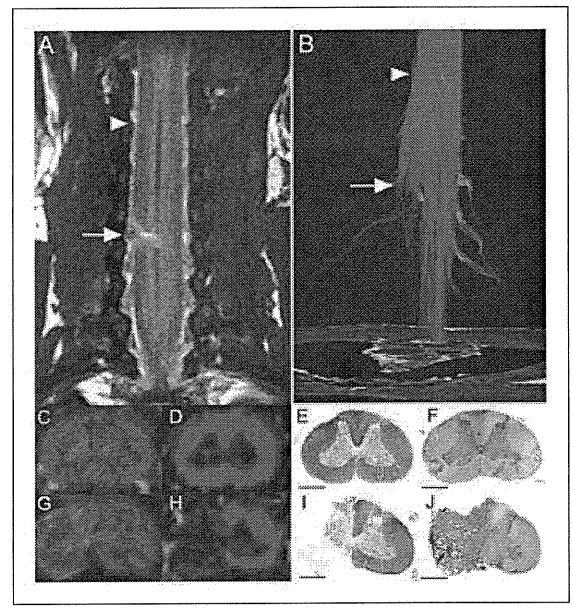

Fig.4 T2WI, DTT, and histological features of a common marmoset with half-cut spinal cord

Cervical segment of the common marmoset spinal cord 2 weeks after it was cut halfway through at the C5/6 level (a post-mortem model). A) MRI T2WI. B) Interrupted nerve fibers of the half-cut spinal cord are visible by DTT. C-F) Spinal cord 2-cm cranial to the half-cut level. G-J) Spinal cord at the half-cut level. Histological features of the HE- (F,J) and LFB- (E,I) stained specimens are well reflected by DTT (C,G) and the colored anisotropy map (D,H). (Reproduced from Reference 26)

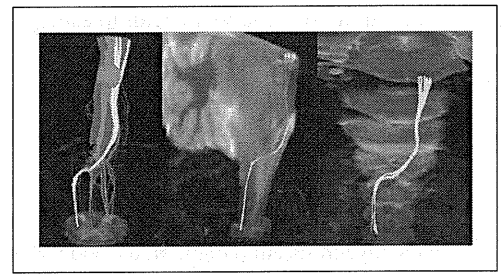

Fig.6 DTT of the corticospinal tract and pyramidal decussation of a common marmoset

The medulla oblongata-pyramidal decussation (an anatomical feature of the corticospinal tract) is clearly depicted in the DTT. In this area, it is known that 90% of corticospinal tract fibers pass through the pyramidal decussation, and a small percentage descend the ipsilateral lateral funiculus (red fibers) or the contralateral anterior funiculus (blue fibers). DTT clearly depicted even these fibers. (Reproduced from Reference 26)

ferent colors according to the direction of their arrangement. Usually, blue is assigned to fibers running longitudinally in the spinal cord, red to fibers running laterally, and green to fibers running dorsoventrally. Fig.3 shows a color FA map of the cross-section of a common marmoset spinal cord. In this figure, the blue represents white matter fibers running vertically[26].

2) Diffusion tensor tractography of the spinal cord

DTT (diffusion tensor tractography) is an imaging technique in which the direction of maximum anisotropy for each voxel is traced. Before spinal DTT can be applied clinically, it is indispensable to conduct detailed analyses to determine the extent to which DTT reflects each tissue type, and the reliability with which DTT depicts axonal information.

With this purpose in mind, we performed DTT for a common marmoset after SCI. Our results yielded the first, worldwide, clear DTT of the spinal cord of an experimental primate. In this experiment, the cervical segment of the spinal cord of a common marmoset was cut halfway through at the C5/6 level, and DTT was performed two weeks later (immediately following the sacrifice of the animal). Unlike MRI, which depicts the injured spinal cord only as changes in signal intensity on T1 and T2 weighted images, DTT allows visualization of the injury in the form of interrupted white matter fibers (Fig.4). The examination of histological specimens stained with HE and LFB confirmed that DTI and DTT precisely reflected the histological features of the injured tissue. By performing detailed post-mortem DTT analyses of this animal model, we devised various ways to minimize artifacts (e.g., movement caused by respiration, the beating of cerebrospinal fluid, etc.), which enabled us to perform spinal cord DTT in live common marmosets. Furthermore, by changing the regions of interest for DTT on the basis of our neuroanatomical findings, we obtained clear projection tract-selective DTT images in live animals (Fig.5). We have also obtained images of the pyramidal decussation, which was previously considered to be impossible (Fig.6)[26]. We have thus demonstrated that DTT is a very useful method of fiber tracking that may replace conventional tracers for monitoring SCI and repair.

Future perspectives

Basic research has been steadily advancing and overcoming the obstacles to the realization of regenerative medicine for SCI. Recently, induced pluripotent stem cells, developed by Yamanaka et al[27], have been attracting considerable attention as a cell source and are expected to provide significant advancements in regenerative medicine. To promote regenerative medicine in Japan and advance its techniques worldwide, further basic research aimed at ascertaining its safety and efficacy, followed by clinical trials, are essential.

References

1) Nakamura M, Bregman BS: Difference in neurotrophic factor gene expression profiles between neonate and adult rat spinal cord after injury. Exp Neurol, 169: 407-415, 2001.
2) Nakamura M, Houghtling RA, MacArthur L, et al: Differences in cytokine expression profile between acute and secondary injury in adult rat spinal cord. Exp Neurol, 184: 313-325, 2003.
3) Okada S, Ishii K, Yamane J, Iwanami A, et al: In vivo imaging of engrafted neural stem cells: its application in evaluating the optimal timing of transplantation for spinal cord injury. FASEB J, 19: 1839-1841, 2005.
4) Ogawa Y, Sawamoto K, Miyata T, et al: Transplantation of in vitro-expanded fetal neural progenitor cells results in neurogenesis and functional recovery after spinal cord contusion injury in adult rats. J Neurosci Res, 69: 925-933, 2002.
5) Iwanami A, Kaneko S, Nakamura M, et al: Transplantation of Human Neural Stem Cells for Spinal Cord Injury in Primates. J Neurosci Res, 80: 182-190, 2005.
6) Le Douarin NM, Kalcheim C: The neural crest UK: Cambridge University Press, 1999.
7) Crane JF, Trainor PA: Neural crest stem and progenitor cells. Annu Rev Cell Dev Biol, 22: 267-286, 2006.
8) Fernandes KJ, McKenzie IA, Mill P, et al: A dermal niche for multipotent adult skin-derived precursor cells. Nat Cell Biol, 6: 1082-1093, 2004.
9) Kruger GM, Mosher JT, Bixby S, et al: Neural crest stem cells persist in the adult gut but undergo changes in self-renewal, neuronal subtype potential, and factor responsiveness. Neuron, 35: 657-669, 2002.
10) Tomita Y, Matsumura K, Wakamatsu Y, et al: Cardiac neural crest cells contribute to the dormant multipotent stem cell in the mammalian heart. J Cell Biol, 170: 1135-1146, 2005.
11) Yoshida S, Shimmura S, Nagoshi N, et al: Isolation of multipotent neural crest-derived stem cells from the adult mouse cornea. Stem cells, 24: 2714-2722, 2006.
12) Yamauchi Y, Abe K, Mantani A, et al: A novel transgenic technique that allows specific marking of the neural crest cell lineage in mice. Dev Biol, 212: 191-203, 1999.
13) Danielian PS, Muccino D, Rowitch DH, et al: Modification of gene activity in mouse embryos in utero by a tamoxifen-

inducible form of Cre recombinase. Curr Biol, 8: 1323-1326, 1998.

14) Kawamoto S, Niwa H, Tashiro F, et al: A novel reporter mouse strain that expresses enhanced green fluorescent protein upon Cre-mediated recombination. FEBS Lett, 470: 263-268, 2000.

15) Nagoshi N, Shibata S, Kubota Y, et al: Multipotent Neural Crest-Derived Stem Cells in Bone Marrow, Dorsal Root Ganglia and Facial Skin. Cell Stem cell, 2: 392-403, 2008.

16) McKenzie IA, Biernaskie J, Toma JG, et al: Skin-derived precursors generate myelinating Schwann cells for the injured and dysmyelinated nervous system. J Neurosci, 26: 6651-6660, 2006.

17) Biernaskie J, Sparling JS, Liu J, et al: Skin-derived precursors generate myelinating Schwann cells that promote remyelination and functional recovery after contusion spinal cord injury. J Neurosci, 27: 9545-9559, 2007.

18) Bixby S, Kruger GM, Mosher JT, et al: Cell-intrinsic differences between stem cells from different regions of the peripheral nervous system regulate the generation of neural diversity. Neuron, 35: 643-656, 2002.

19) Sieber-Blum M, Schnell L, Grim M, et al: Characterization of epidermal neural crest stem cell (EPI-NCSC) grafts in the lesioned spinal cord. Mol Cell Neurosci, 32: 67-81, 2006.

20) GrandPre T, Li S, Strittmatter SM: Nogo-66 receptor antagonist peptide promotes axonal regeneration. Nature, 417: 547-551, 2002.

21) Bradbury EJ, Moon LD, Popat RJ et al: Chondroitinase ABC promotes functional recovery after spinal cord injury. Nature, 416: 636-640, 2002.

22) Ellezam B, Dubreuil C, Winton M et al: Inactivation of intracellular Rho to stimulate axon growth and regeneration. Prog Brain Res, 137: 371-380, 2002.

23) Fournier AE, Takizawa BT, Strittmatter SM. Rho kinase inhibition enhances axonal regeneration in the injured CNS. J Neurosci, 23: 1416-1423, 2003.

24) Kaneko S, Iwanami A, Nakamura M, et al: Axonal Regeneration and Functional Recovery by Administration of Strong and Selective Semaphorin3A Inhibitor into the Injured Spinal Cord. Nat Med, 12: 1380-1389, 2006.

25) Ikegami T, Nakamura M, Yamane J, et al: Chondroitinase ABC combined with neural stem/progenitor cell transplantation enhances graft cell migration and outgrowth of GAP-43-positive fibers after rat spinal cord injury. Euro J Neurosci, 2: 3036-3046, 2005.

26) Fujiyoshi K, Yamada M, Nakamura M, et al: In vivo tracing of neural tracts in the intact and injured spinal cord of marmosets by diffusion tensor tractography. J Neurosci, 27: 11991-11998, 2007.

27) Takahashi K, Yamanaka S: Induction of pluripotent stem cells from mouse embryonic and adult fibroblast cultures by defined factors. Cell, 126: 663-676. 2006.

Review Article

Toward using iPS cells to treat spinal cord injury: Their safety and therapeutic efficacy

Kyoko Miura[1)], Osahiko Tsuji[1,2)], Masaya Nakamura[2)] and Hideyuki Okano[1,*)]

1) Department of Physiology, School of Medicine, Keio University, Tokyo, Japan.

2) Department of Orthopedics, School of Medicine, Keio University, Tokyo, Japan.

The spinal cord, which is part of the central nervous system, has been considered a typical example of an organ in which regeneration is difficult. However, since the report of recovery of function in a spinal cord injury (SCI) model as a result of cell transplantation of rat-fetus-derived neural stem/progenitor cells (NS/PCs), stem cell transplantation therapy has attracted great hope of restoring and replenishing lost neurons and glia.

In recent years induced pluripotent stem (iPS) cells that possess embryonic stem (ES)-cell-like pluripotency and proliferative capacity have been produced by introducing several different genes into somatic cells. Rapid progress is currently being made in research on iPS cells with the aim of enabling cell transplantation therapy, and reports of the development of methods of inducing human iPS cells to differentiate into a variety of somatic cells and cases of treatment of murine models with mouse iPS cells have appeared one after another. However, when viewed from a safety standpoint, problems that arise because ES cells and iPS cells are both pluripotent stem cells and many problems unique to iPS cells, which have been artificially reprogrammed, still remain unresolved, and there is a desire for further progress in research. In this paper we outline these issues and report the latest findings in regard to application to the treatment of spinal cord injury.

Rec./Acc.11/24/2010

*Corresponding author: Department of Physiology, School of Medicine, Keio University, 35 Shinanomachi, Shinjuku-ku, Tokyo, 112-0012, Japan.
Tel: +81-3-5363-3746, Fax: +81-3-3357-5445, e-mail: hidokano@a2.keio.jp

Key words: iPS cells (induced pluripotent stem cells), neural differentiation, cell transplantation, tumor formation, spinal cord injury, safety

Introduction

According to the rapid progress of iPS cell researches[1-6], on June 30, 2010, a revision of the Japanese Ministry of Health, Labour and Welfare's Guidelines for Clinical Research Using Human Stem Cells was adopted by a committee, and clinical research involving the use of induced pluripotent stem cells (iPS cells), irrespective of whether homologous or heterologous, is now covered by the guidelines. The revised guideline was launched on November 1, 2010. That appears to be a major step in terms of the future development of regenerative medicine in Japan. However, fetal stem cells and embryonic stem (ES) cells are still not covered by the guidelines. The clinical trials of human ES cells-based therapy has already started in the United States in October, 2010.

The central nervous system (CNS), including brain and spinal cord, has been considered a representative example of organs in which regeneration is difficult. However, the situation has been changing based on the fact that several groups, including our own, have demonstrated that stem cells are also present in the adult CNS of mammals, including humans, and that neurogenesis occurs in the brains of adults[7-9]. The regeneration of CNS regeneration means three things: (i) axon regeneration, (ii) replenishment of cells that have been lost as a result of disease, and (iii) functional recovery[10]. It seems that a strategy based on the fundamental concept of inducing recapitulation of developmental process will definitely be necessary in order to realize the CNS-regeneration. In the fall of 2006, a Keio University–Kyoto University Joint Research Team was established as a result of the close collaboration between our research group and Professor Shinya Yamanaka's research laboratory, with the aim of applying iPS cells to the treatment of SCI. In this paper we describe basic research and the current situation in relation to iPS cells with the aim of regenerative medicine for the CNS, and we discuss future prospects.

(1) Tasks common to both iPS cells and ES cells

a) Tasks related to tumor (teratoma) formation by undifferentiated cells that persist after induction of differentiation

ES cells are endowed with both semipermanent proliferative capacity and pluripotency, i.e., the ability to differentiate into a variety of different cell types, and iPS cells possess properties that resemble ES cells in these two respects. Transplanting cells obtained after inducing these pluripotent stem cells to differentiate into the target cells is regarded as the usual method of applying them to cell transplantation therapy. However, a problem arises when this is done, because of teratoma formation caused by undifferentiated cells that remain after the induction of differentiation. We produced neurospheres containing neural stem/progenitor cells (NS/PCs) from mouse ES cells and iPS cells and assessed their safety by transplanting them into the striatum of non-obese/severe combined immunodeficient (NOD/SCID) mice[11]. The results showed that teratomas had been formed by intermingled undifferentiated cells in 10% of the group of mice into which ES-cell-derived neurospheres had been transplanted and in 40% of the group of mice into which iPS-cell-derived neurospheres had been transplanted. It has been reported that teratoma formation can be avoided by transplanting cells induced to differentiate into NS/PCs from mouse ES cells after using expression of the neural stem/progenitor cell marker Sox1 to purify them[12]. Jaenisch et al. reported that no teratoma formation occurred when they induced the formation of dopaminergic neurons from mouse iPS cells and transplanted them after eliminating cells that were positive for theundifferentiated-cell-marker SSEA-1 with a flowcytometer[5]. It seems important to establish methods of inducing differentiation that yield highly pure target cells, and to develop flowcytometers that comply with Good Manufacturing Practice (GMP) grade

and target cell purification methods that make full use of them.

b) Tasks regarding the safety of differentiated cell transplantation

Even if it is possible to avoid the risk of teratoma formation as discussed in (i), the possibility of tumor formation after transplantation of differentiated cells must be assessed long-term and carefully. In 2008, the development of a transplanted-cell-derived brain tumor was reported in a boy with ataxia telangiectasia who had undergone intracerebral transplantation of human fetal neural stem cells[13]. There are great expectations of trials of transplantation of NS/PCs differentiated from human iPS cells or ES cells as a method of treating SCI, Parkinson's disease, etc., but, depending on the circumstances, assessment of treatments that use growth-arrested cells, or novel methods to ensure safety may become necessary, e.g., introducing a suicide gene such as HSV-TK in advance so that it is possible to eliminate the transplanted cells in the worst case scenario.

(2) Tasks peculiar to iPS cells

a) Tasks from a safety standpoint as a result of introducing genes

iPS cells were initially produced by introducing four factors, i.e., Oct3/4, Klf4, c-Myc, and Sox2, by means of retrovirus vectors. c-Myc is well known as a proto-oncogene, and the other three factors are genes that are known to be highly expressed in cancer. The probability that tumors would develop in chimeric mice and their progeny produced as a result of using these four-factor iPS cells was found to be approximately 20%[14]. Because expression of c-Myc transgene that had been integrated into the genome of iPS cells with the retrovirus became reactivated in these tumors, the risk resulting from the transduction of c-Myc became a problem. However, it was later discovered that, although the rate is low, iPS cells could be generated by introducing the other three factors without c-Myc[15], and no tumors were detected in the chimeric mice produced with the iPS cells derived with the three factors even when they were observed for more than 100 days. At that point the production of iPS cells without using c-Myc had been achieved, but the problems associated with the other three factors having been inserted into the genome with retroviruses had not been resolved. Retroviruses and lentiviruses are often integrated in proximity to a gene promoter, and there is the risk that they will alter the state of expression of endogenous genes in the vicinity and cause tumorigenesis. Development of leukemia in 2 of 10 patients with X-linked severe combined immunodeficiency (X-SCID) who underwent gene therapy with a retrovirus vector has actually been reported[16]. There has been rapid progress in research on this problem in recent years, and success without using retroviruses or lentiviruses has been reported in regard to production of so called "integration free iPS cells" (i.e., iPS cells into whose genome no exogenous genes have been inserted) by using the transducing proteins[17,18], a plasmid or an episomal vector[19,20], Sendai virus vector[21] and in vitro synthesized RNA[22]. It appears to be desirable to use the integration-free iPS cells, when using cell transplantation therapy. Nevertheless, in the future detailed comparisons of their properties will be necessary to determine whether the integration-free iPS cells produced by these methods possess pluripotency and in vitro differentiation capacity comparable to that of iPS cells produced with retroviruses.

b) Tasks from a safety standpoint associated with the reprogramming of somatic cells and the type of original cells

Somatic cell nuclear transfer (SCNT) to oocytes is known as other reprogramming methods besides induction of iPS cells. The birth rate of clone mice produced by SCNT is very low, and such abnormalities as placental hyperplasia, obesity, and a short life span

have been discovered and are thought to be attributable to inadequate reprogramming of the somatic cell nuclei. On the other hand, hardly any differences in gene expression or DNA methylation status have been found between ntES (ES cells produced from cloned blastocysts after SCNT)[23] and ordinary ES cells, and production of tetraploid chimeras is also possible. Production of tetraploid chimeras from iPS cells has also been reported recently[24], and in that respect iPS cells appear to have capacities that are fairly close to those of ES cells. However, gene expression in iPS cells and ES cells is not the same, and there are even reports that part of the gene expression patterns of the cells from which they were derived persists[25]. Moreover, we recently discovered that the response of iPS cells to inductive signals of differentiation and tumorigenic propensities vary with the type of somatic cells from which they were derived (see below). Based on these findings there is a strong possibility that some of the properties of the original somatic cells persist in iPS cells, and when they are used for cell transplantation therapy the possibility of causing tumor formation or some other form of abnormality cannot be ruled out. Because many genes are thought to be involved in somatic cell reprogramming, it may be possible to produce better quality iPS cells by increasing the number of reprogramming factors. There are high hopes that future progress in research will reveal the optimal composition of the reprogramming cocktail.

We recently demonstrated that the responsiveness of iPS cells to neural differentiation and their safety after transplantation vary greatly according to differences in somatic cell origin at the time they were generated[11]. We induced differentiation of neurospheres by using 36 mouse iPS cell clones that had previously been generated in our laboratory, and then evaluated their differentiation capacity in vitro and safety after transplantation by transplanting them into the striatum of the brains of NOD/SCID mice. The results showed that almost all of the iPS cell lines analyzed were capable of differentiating into neurospheres. However, a detailed analysis by flowcytometry showed large differences in the percentages of Nanog-EGFP-positive undifferentiated cells that remained in the neurospheres according to the type of somatic cells from which the iPS cells had been derived. A mouse embryonic fibroblast (MEF)-derived iPS cell clone showed responsiveness to induction of differentiation that was comparable to that of ES cells, and hardly any undifferentiated cells remained in the neurospheres. Teratoma formation after transplantation in a group of mice transplanted with neurospheres derived from this MEF-iPS cell clone was infrequent and minor, and it was comparable to the results in a group of mice transplanted with ES-cell-derived neurospheres. Moreover, no teratoma formation was observed during a 16-week observation period in a group transplanted with two iPS cell clones that had been produced from adult gastric epithelial cells (Stm). On the other hand, an iPS cell clone derived from adult tail-tip fibroblasts (TTFs) showed statistically significant resistance to differentiation, and many undifferentiated cells remained in the neurospheres after inducing differentiation. Formation of significantly larger teratomas was observed in the group of mice into which these TTF-iPS-derived neurospheres had been transplanted, and many of the mice soon became debilitated or died. The responsiveness to induction of differentiation and the tumor formation capacity of an adult hepatocytes (Hep)-derived iPS cell clone were intermediate between that of the MEF-iPS cell clone and TTF-iPS cell clone. On the other hand, whether c-Myc had been introduced or screening of the reprogrammed cells by means of reporter proteins had been performed at the time they were generated had no effect on the responsiveness of the iPS cells to induction of differentiation or on their safety after transplantation. It appears that persistence of the gene expression patterns of the original somatic cells from which they were derived, as stated

above, may be the reason why variations in the differentiation capacity of the iPS cells emerged according to differences in the cells from which they were derived. In connection with this, according to a recent report, early-passage iPS cells obtained by reprogramming adult mouse tissue by means of transcription factors, leave behind traces of characteristic DNA methylation in the original somatic cell tissue. They show a tendency to differentiate along cell lineages similar to the donor cells, and choices of any other cell fates are narrowed. This sort of donor tissue "epigenetic memory" has been reported to play a large role in the properties of iPS cells. Moreover, Dr. Kazuhiro Sakurada has proposed calling genes whose expression pattern in iPS cells and ES cells is different "reprogramming-recalcitrant genes"[26]. This name is based on these genes showing resistance to the same transcription status being induced as in ES cells. Identifying "reprogramming-recalcitrant genes" that are the cause of tumor formation by neural cells derived from iPS cells is definitely important in the future.

(3) Transplantation of "safe" mouse iPS-cell-clone-derived neural stem cells to treat SCI

The therapeutic effects of NS/PCs-transplantation in the treatment of SCI has been reported many times at the research level. Our own laboratory has also previously reported the effectiveness of rodent fetal NS/PCs or ES-derived NS/PCs in the treatment of SCI[27-30] and the effectiveness of human NS/PCs-transplantation in a primate common marmoset model of SCI[31-32]. Because the cells used for transplantation in these studies were derived from fetuses, it is difficult to proceed with clinical application because of the ethical issue. It appears that this ethical issue can be avoided by using iPS-cell-derived NS/PCs.

We therefore first assessed safety by in vivo transplantation into the brains of the NOD/SCID mice described above, and then conducted a study of effectiveness by transplanting neurospheres derived from a mouse iPS cell clone whose safety had been confirmed into a model of contusive SCI[33]. Neurosphere transplantation was performed in the subacute stage on day 9 after the injury. The results of bioimaging with luciferase showed that approximately 20% of the transplanted neurospheres had survived in the injured spinal cord, and they had differentiated into the three neural lineages. Severe atrophic change and demyelination had occurred in the injured spinal cord after the contusive injury, but these changes were significantly prevented in the group transplanted with iPS-cell-derived neurospheres. When hindlimb motor function was evaluated by the Basso mouse scale, significantly better recovery of function was seen in the group transplanted with iPS-cell-derived neurospheres than in the control groups (phosphate-buffered saline [PBS] transplanted group and fibroblast transplanted group). This recovery of function appeared to have been due to such effects as promotion of axonal growth in the raphespinal serotonergic fibers, which are associated with locomotor functions of hindlimbs, and remyelination by the transplanted cells-derived oligodendrocytes, in addition to the prevention of atrophic change and demyelination described above.

Next, we conducted a similar transplantation experiment using adult-tissue (TTF)--derived iPS cell clones as a more realistic clinical application model. Only one of the six TTF-derived iPS cell clones used in the safety study described above was safe, and after inducing differentiation into neurospheres of this one "safe" TTF-derived iPS cell clone and two "unsafe" TTF-derived iPS cell clones that had been found capable of tumor formation, we transplanted them into a mouse model of SCI. The results showed that although recovery of function was seen in the all of the groups into which TTF-iPS-clone-derived neurospheres had been transplanted, the function recovery that had been temporarily attained in the groups transplanted with

"unsafe" TTFiPSclonederived neurospheres was suddenly lost 6 weeks after the injury due to the tumor mass effects, and most to the mice suddenly died. Furthermore, no tumor formation was seen in the group into which "safe" TTFiPS-clone-derived neurospheres had been transplanted, and recovery of function recovery had obviously been achieved. Based on these findings, it was shown that although there is a great deal of variation among iPS cell clones in regard to safety after transplantation, if safety is rigorously assessed in advance, they are capable of serving as a source of cells that are useful for treating SCI.

(4) Future tasks and prospects

As shown above, iPS cells can be said to have great potential as a cell transplantation source for the treatment of SCI. However, their safety, i.e., the "quality" of iPS cells, must be evaluated very carefully.

At present, the methods that are generally used to evaluate iPS cells that have been generated consist of (1) transplanting cells in an undifferentiated state subcutaneously or into the testes of mice and assessing their ability to differentiate into cell types of the three embryonic germ layers in vivo by allowing them to form teratomas, (2) assessing their degree of contribution to chimeric mice and their degree of contribution to germline transmission by transplanting undifferentiated cells into blastocysts (impossible to apply to human iPS cells), (3) analysis of global gene expression by means of microarrays, and (4) genome analysis by karyotyping or comparative genomic hybridization (CGH) arrays. However, it may be impossible to adequately evaluate the safety of iPS cells by these methods alone. Our research has revealed that evaluation by in vitro differentiation induction systems is also very important. iPS cell clones that contribute to the germline of chimeric mice are not always highly responsive to induction of differentiation in vitro. On the other hand, almost all iPS cells clones with poor responsiveness to induction of differentiation and that form large teratomas after transplantation have been able to contribute to chimeric mice. These findings clearly show that it is impossible to evaluate the quality or safety of iPS cells by means of just one evaluation system, and evaluation from multiple angles is essential. iPS cells have the advantage of being able to conveniently establish many clones, but at the same time it has been becoming clear that there are large variations in quality between the clones. It appears that picking out the highest quality clone from a number of iPS cell clones that have been established from individual patients is a necessary task, but evaluating each of the clones from many different aspects including karyotypes, flowcytometric analysis, gene expression profile, whole genome methylation patterns and tumorigenic propensities of NS/PCs derived from them, is extremely unrealistic in terms of both time and cost. It seems that a screening system that makes it possible to conveniently separate out good quality clones will need to be established in the future. It was recently reported that there is a correlation between the potential of ES/iPS cells for germline transmission and ability to contribute to tetraploid chimeras and the activity of the Dlk1-Dio3 imprinted gene cluster on mouse chromosome[12, 34, 35]. However, as stated above, there is a strong possibility that the markers of potential for germline transmission and ability to contribute to chimera mice and the markers of ability to differentiate in vitro are different. Moreover, which differentiated cells to produce and what to use them for, and the criteria that they will have to meet are expected to differ even more according to their intended purpose. It seems that it will be necessary to search for a variety of markers that will serve as indicators of responsiveness to induction of differentiation that is suited to each individual purpose.

The generation of iPS cells is an extremely large first step toward making cell transplantation therapy with self-derived pluripotent stem cells a reality. In view of the cur-

rent rate of progress in iPS cell research worldwide, we have the feeling that the day when iPS cells will actually be applied to transplantation therapy of SCI is not very far off. However, as stated in this article, many tasks regarding safety when iPS cells are applied to transplantation therapy remain, and when they have been resolved it will be possible to administer them to humans for the first time. It is important to proceed with research in a multifaceted manner while conducting careful evaluations. In addition to research directly linked to clinical applications and to basic research with a view to clinical applications, it appears important to freely proceed with a variety of basic research, to vigorously debate the information obtained, and to integrate it.

Acknowledgments

The original work described in the present review article was done in collaboration with Professors Shinya Yamanaka at Kyoto University and Yoshiaki Toyama at Keio University. This work was supported by grants from the Ministry of Education, Culture, Sports, Science and Technology of Japan (MEXT), the project for realization of regenerative medicine and support for the core institutes for iPS cell research from MEXT and a Grant-in-aid for the Global COE program from MEXT to Keio University. Authors have no financial conflict of interests related to this work.

References

1) Takahashi K, Yamanaka S: Induction of pluripotent stem cells from mouse embryonic and adult fibroblast cultures by defined factors. Cell. 2006; 126: 663-676.

2) Takahashi K, Tanabe K, Ohnuki M, Narita M, Ichisaka T, Tomoda K, Yamanaka S: Induction of pluripotent stem cells from adult human fibroblasts by defined factors. Cell. 2007; 131: 861-872.

3) Yu J, Vodyanik MA, Smuga-Otto K, Antosiewicz-Bourget J, Frane JL, Tian S, Nie J, Jonsdottir GA, Ruotti V, Stewart R, Slukvin II, Thomson JA: Science. 2007; 318: 1917-1920.

4) Hanna J, Wernig M, Markoulaki S, Sun CW, Meissner A, Cassady JP, Beard C, Brambrink T, Wu LC, Townes TM, Jaenisch R: Treatment of sickle cell anemia mouse model with iPS cells generated from autologous skin. Science. 2007; 318: 1920-1923.

5) Wernig M, Zhao JP, Pruszak J, Hedlund E, Fu D, Soldner F, Broccoli V, Constantine-Paton M, Isacson O, Jaenisch R: Neurons derived from reprogrammed fibroblasts functionally integrate into the fetal brain and improve symptoms of rats with Parkinson's disease.Proc. Natl. Acad. Sci. USA. 2008; 105: 5856-5861.

6) Ellis J, Baum C, Benvenisty N, Mostoslavsky G, Okano H, Stanford WL, Porteus M, Sadelain M: Benefits of utilizing gene-modified iPSCs for clinical applications. Cell Stem Cell. 2010; 7: 429-430.

7) Roy NS, Wang S, Jiang L, Kang J, Benraiss A, Harrison-Restelli C, Fraser RA, Couldwell WT, Kawaguchi A, Okano H, Nedergaard M, Goldman SA: In vitro neurogenesis by progenitor cells isolated from the adult human hippocampus. Nature Medicine 2000; 6: 271-277.

8) Okano H, Sawamoto K: Neural Stem Cells: Involvement in Adult Neurogenesis and CNS Repair. Philos Trans R Soc Lond B Biol Sci. 2008; 363, 2111-2122.

9) Okano H: Neural stem cells and strategies for the regeneration of the central nervous system. Proc. Jpn. Acad., Ser. B 2010; 86: 438-450.

10) Okano H: Making and repairing the mammalian brain: Introduction. Semin Cell Dev Biol. 2003; 14: 159.

11) Miura K, Okada Y, Aoi T, Okada A, Takahashi K, Okita K, Nakagawa M, Koyanagi M, Tanabe K, Ohnuki M, Ogawa D, Ikeda E, Okano H, Yamanaka S: Variation in the safety of inducedpluripotent stem cell lines Nature Biotechnol. 2009; 27: 743-745.

12) Fukuda H, Takahashi J, Watanabe K, Hayashi H, Morizane A, Koyanagi M, Sasai Y, Hashimoto N: Fluorescence-activated cell sorting-based purification of embryonic stem cell-derived neural precursors averts tumor formation after transplantation.Stem Cells 2006; 24: 763-771.

13) Amariglio N, Hirshberg A, Scheithauer BW, Cohen Y, Loewenthal R, Trakhtenbrot L, Paz N, Koren-Michowitz M, Waldman D, Leid-

er-Trejo L, Toren A, Constantini S, Rechavi G: Donor-derived brain tumor following neural stem cell transplantation in an ataxia telangiectasia patient. PLoS Med. 2009; 6: e1000029.

14) Okita K, Ichisaka T, Yamanaka S: Generation of germline-competent induced pluripotent stem cells. Nature. 2007; 448: 313-317.

15) Nakagawa M, Koyanagi M, Tanabe K, Takahashi K, Ichisaka T, Aoi T, Okita K, Mochiduki Y, Takizawa N, Yamanaka S: Generation of induced pluripotent stem cells without Myc from mouse and human fibroblasts. Nat Biotechnol. 2008; 26: 101-106.

16) Hacein-Bey-Abina S, Von Kalle C, Schmidt M, McCormack MP, Wulffraat N, Leboulch P, Lim A, Osborne CS, Pawliuk R, Morillon E, Sorensen R, Forster A, Fraser P, Cohen JI, de Saint Basile G, Alexander I, Wintergerst U, Frebourg T, Aurias A, Stoppa-Lyonnet D, Romana S, Radford-Weiss I, Gross F, Valensi F, Delabesse E, Macintyre E, Sigaux F, Soulier J, Leiva LE, Wissler M, Prinz C, Rabbitts TH, Le Deist F, Fischer A, Cavazzana-Calvo M: LMO2-associated clonal T cell proliferation in two patients after gene therapy for SCID-X1. Science, 2003; 302: 415-419.

17) Zhou H, Wu S, Joo JY, Zhu S, Han DW, Lin T, Trauger S, Bien G, Yao S, Zhu Y, Siuzdak G, Schöler HR, Duan L, Ding S: Generation of induced pluripotent stem cells using recombinant proteins. Cell Stem Cell. 2009; 4: 381-384.

18) Kim D, Kim CH, Moon JI, Chung YG, Chang MY, Han BS, Ko S, Yang E, Cha KY, Lanza R, Kim KS: Generation of human induced pluripotent stem cells by direct delivery of reprogramming proteins. Cell Stem Cell. 2009; 4 : 472-476.

19) Okita K, Nakagawa M, Hyenjong H, Ichisaka T, Yamanaka S: Generation of mouse induced pluripotent stem cells without viral vectors. Science. 2008; 322: 949-953.

20) Yu J, Hu K, Smuga-Otto K, Tian S, Stewart R, Slukvin II, Thomson JA: Human induced pluripotent stem cells free of vector and transgene sequences. Science. 2009; 324 : 797-801.

21) Fusaki N, Ban H, Nishiyama A, Saeki K, Hasegawa M: Efficient induction of transgene-free human pluripotent stem cells using a vector based on Sendai virus, an RNA virus that does not integrate into the host genome. Proc Jpn Acad Ser B Phys Biol Sci. 2009; 85: 348-362.

22) Warren L, Manos PD, Ahfeldt T, Loh YH, Li H, Lau F, Ebina W, Mandal PK, Smith ZD, Meissner A, Daley GQ, Brack AS, Collins JJ, Cowan C, Schlaeger TM, Rossi DJ: Highly efficient reprogramming to pluripotency and directed differentiation of human cells with synthetic modified mRNA. . Cell Stem Cell. 2010; 7: 618-630.

23) Wakayama T. et al.: Differentiation of embryonic stem cell lines generated from adult somatic cells by nuclear transfer. Science. 2001; 292: 740-743.

24) Zhao XY, Li W, Lv Z, Liu L, Tong M, Hai T, Hao J, Guo CL, Ma QW, Wang L, Zeng F, Zhou Q: iPS cells produce viable mice through tetraploid complementation. Nature. 2009; 461: 86-90.

25) Kim K, Doi A, Wen B, Ng K, Zhao R, Cahan P, Kim J, Aryee MJ, Ji H, Ehrlich LI, Yabuuchi A, Takeuchi A, Cunniff KC, Hongguang H, McKinney-Freeman S, Naveiras O, Yoon TJ, Irizarry RA, Jung N, Seita J, Hanna J, Murakami P, Jaenisch R, Weissleder R, Orkin SH, Weissman IL, Feinberg AP, Daley GQ: Epigenetic memory in induced pluripotent stem cells. Nature. 2010; 467: 285-290.

26) Sakurada K: Environmental epigenetic modifications and reprogramming recalcitrant genes. Stem Cell Res. 2010; 4:157-164.

27) Okano H: The stem cell biology of the central nervous system. J. Neurosci. Res. 69: 2002; 69: 698-707.

28) Ogawa Y, Sawamoto K, Miyata T, Miyao S, Watanabe M, Nakamura M, Bregman BS, Koike M, Uchiyama Y, Toyama Y, Okano H: Transplantation of in vitro-expanded fetal neural progenitor cells results in neurogenesis and functional recovery after spinal cord contusion injury in adult rats. J. Neurosci. Res. 2002; 69: 925-933.

29) Okada S, Ishii K, Yamane J, Iwanami A, Ikegami T, Iwamoto Y, Nakamura M, Miyoshi H, Okano HJ, Contag CH, Toyama Y, Okano H: In vivo imaging of engrafted neural stem cells: its application inevaluating the optimal timing of transplantation for spinal cord injury. FASEB J. 2005; 19: 1839-1841.

30) Kumagai G, Okada Y, Yamane J, Kitamura K, Nagoshi N, Mukaino M, Tsuji O, Fujiyoshi K, Okada S, Shibata S, Toh S, Toyama Y, Nakamura M, Okano H: Roles of ES cell-derived gliogenic neural stem/progenitor cells in functional recovery after spinal cord injury. PLOS ONE 2009; 4: e7706.

31) Iwanami A, Yamane J, Katoh H, Nakamura

M, Momomoshima S, Ishii H, Tanioka Y, Tamaoki N, Nomura T, Toyama Y, Okano H: Establishment of Graded Spinal Cord Injury Model in a Non-human Primate: the Common Marmoset. J. Neurosci,Res. 2005; 80: 172-181.

32) Iwanami A, Kakneko S, Nakamura M, Kanemura Y, Mori H, Kobayashi S, Yamasaki M, Momoshima S, Ishii H, Ando K, Tanioka Y, Tamaoki N, Nomura T, Toyama Y, Okano H: Transplantation of human neural stem/progenitor cells promotes functional recovery after spinal cord injury in common marmoset. J. Neurosci, Res. 2005; 80: 182-190.

33) Tsuji O, Miura K, Okada Y, Fujiyoshi K, Nagoshi N, Kitamura K, Kumagai G, Mukaino M, Nishino M, Tomisato S, Higashi H, Ikeda E, Nagai T, Kohda K, Takahashi K, Okita K, Katoh H, Matsuzaki Y, Yuzaki M, Toyama Y, Nakamura M, Yamanaka S, Okano H: Therapeutic effect of the appropriatelly evaluated 'safe' iPS cells for spinal cord injury. Proc.Natl.Acad.Sci.USA 2010; 107: 12704-12709.

34) Stadtfeld M, Apostolou E, Akutsu H, Fukuda A, Follett P, Natesan S, Kono T, Shioda T, Hochedlinger K: Aberrant silencing of imprinted genes on chromosome 12qF1 in mouse induced pluripotent stem cells. Nature. 2010; 465: 175-181.

35) Liu L, Luo GZ, Yang W, Zhao X, Zheng Q, Lv Z, Li W, Wu HJ, Wang L, Wang XJ, Zhou Q: Activation of the imprinted Dlk1Dio3 region correlates with pluripotency levels of mouse stem cells. J Biol Chem. 2010; 285: 19483-19490.

Infection and Immunity

Establishment of a Real-Time, Quantitative, and Reproducible Mouse Model of Staphylococcus Osteomyelitis Using Bioluminescence Imaging

Haruki Funao, Ken Ishii, Shigenori Nagai, Aya Sasaki, Tomoyuki Hoshikawa, Mamoru Aizawa, Yasunori Okada, Kazuhiro Chiba, Shigeo Koyasu, Yoshiaki Toyama and Morio Matsumoto

Infect. Immun. **2012, 80(2):733. DOI: 10.1128/IAI.06166-11. Published Ahead of Print 21 November 2011.**

IAI
Journals.ASM.org

Establishment of a Real-Time, Quantitative, and Reproducible Mouse Model of Staphylococcus Osteomyelitis Using Bioluminescence Imaging

Haruki Funao,[a] Ken Ishii,[a,f] Shigenori Nagai,[b,c] Aya Sasaki,[d] Tomoyuki Hoshikawa,[e] Mamoru Aizawa,[e,f] Yasunori Okada,[d] Kazuhiro Chiba,[a] Shigeo Koyasu,[b] Yoshiaki Toyama,[a] and Morio Matsumoto[a,f]

Department of Orthopaedic Surgery, School of Medicine, Keio University, Shinjuku, Tokyo, Japan[a]; Department of Microbiology and Immunology, School of Medicine, Keio University, Shinjuku, Tokyo, Japan[b]; Core Research for Evolutional Science and Technology (CREST), Japan Science and Technology Agency (JST), Tokyo, Japan[c]; Department of Pathology, School of Medicine, Keio University, Shinjuku, Tokyo, Japan[d]; Department of Applied Chemistry, School of Science and Technology, Meiji University, Ikuta, Kanagawa, Japan[e]; and Kanagawa Academy of Science and Technology (KAST), Kawasaki, Kanagawa, Japan[f]

Osteomyelitis remains a serious problem in the orthopedic field. There are only a few animal models in which the quantity and distribution of bacteria can be reproducibly traced. Here, we established a real-time quantitative mouse model of osteomyelitis using bioluminescence imaging (BLI) without sacrificing the animals. A bioluminescent strain of *Staphylococcus aureus* was inoculated into the femurs of mice. The bacterial photon intensity (PI) was then sequentially measured by BLI. Serological and histological analyses of the mice were performed. The mean PI peaked at 3 days, and stable signals were maintained for over 3 months after inoculation. The serum levels of interleukin-6, interleukin-1β, and C-reactive protein were significantly higher in the infected mice than in the control mice on day 7. The serum monocyte chemotactic protein 1 level was also significantly higher in the infected group at 12 h than in the control group. A significantly higher proportion of granulocytes was detected in the peripheral blood of the infected group after day 7. Additionally, both acute and chronic histological manifestations were observed in the infected group. This model is useful for elucidating the pathophysiology of both acute and chronic osteomyelitis and to assess the effects of novel antibiotics or antibacterial implants.

One of the most serious problems in the orthopedic field is infectious osteomyelitis, which causes progressive inflammation and destruction of bone tissue (19). Treatment of infectious osteomyelitis is challenging, because the pathogenic organisms and their drug sensitivities are variable. This problem is compounded by increasing numbers of drug-resistant bacterial strains, implant-associated infections, and elderly patients with compromised immune systems (18). Although progress has been made, controlling infectious osteomyelitis is still difficult. Therefore, experimental studies are warranted to develop more effective treatment options. A number of animal models of osteomyelitis have been reported (13, 26, 33, 35). However, many of them require sacrifice of the animals, and thus, they are limited in their availability for real-time assessments of the severity of infection and the efficacy of treatments. As a result, the pathophysiology of osteomyelitis remains poorly understood.

A recent development in optical imaging, bioluminescence imaging (BLI), permits the noninvasive sequential monitoring of cell growth and gene expression *in vivo*. This method allows real-time monitoring of implanted cells in live animals (16, 27). Inoculated bacteria that emit a constant bioluminescent signal can be detected through the tissues of a live animal using an ultrasensitive, cooled, charge-coupled device (CCD) camera. This approach has proven useful in studies in the fields of oncology (38), endocrine disruptors (28), metabolism (37), hematopoietic cells (41), regenerative medicine (16, 27), immunology (6, 21), and infections (2, 5, 11, 14, 20, 24, 34, 42).

Previous models of infectious diseases required sacrifice of animals to quantify the bacteria by culturing tissue specimens. In contrast, the BLI technique monitors bacterial growth throughout the course of infection in real time without sacrificing animals. To our knowledge, there is no previous model in which infectious processes in bone from the acute to the chronic phases were evaluated using BLI, as well as the kinetics of immune cells and the levels of cytokines/chemokines in serum. The purpose of the present study was to establish a real-time, quantitative, and reproducible mouse model of osteomyelitis using the BLI technique.

MATERIALS AND METHODS

Bioluminescent bacteria. A bioluminescent strain of *Staphylococcus aureus*, Xen-29, was obtained from Caliper LS Co. (Hopkinton, MA) and cultured in Luria Bertani medium (Sigma-Aldrich Co., St. Louis, MO) at 37°C under ambient aeration with gentle agitation. The bacteria were selectively grown in medium containing 200 μg/ml kanamycin. *S. aureus* Xen-29, derived from the parental strain ATCC 12600, has a stable copy of a modified *Photorhabdus luminescens luxABCDE* operon, encoding enzymes responsible for the luminescent reaction. Bacterial bioluminescence requires no substrate to be added to generate the light and will constitutively emit a bioluminescent signal as long as the organism is viable. The bacterial samples were frozen and stored at −80°C. The samples were thawed at 4°C for 1 h prior to each experiment. Typically, bacterial viability was maintained at 4°C for approximately 5 h after thawing.

Mouse osteomyelitis model. Eighteen BALB/c adult male mice (12 weeks old; 20 to 25 g) purchased from Sankyo Labo Service (Shizuoka,

Received 10 November 2011 Accepted 10 November 2011
Published ahead of print 21 November 2011
Editor: A. J. Bäumler
Address correspondence to Ken Ishii, ishii-km@sc.itc.keio.ac.jp.

doi:10.1128/IAI.06166-11

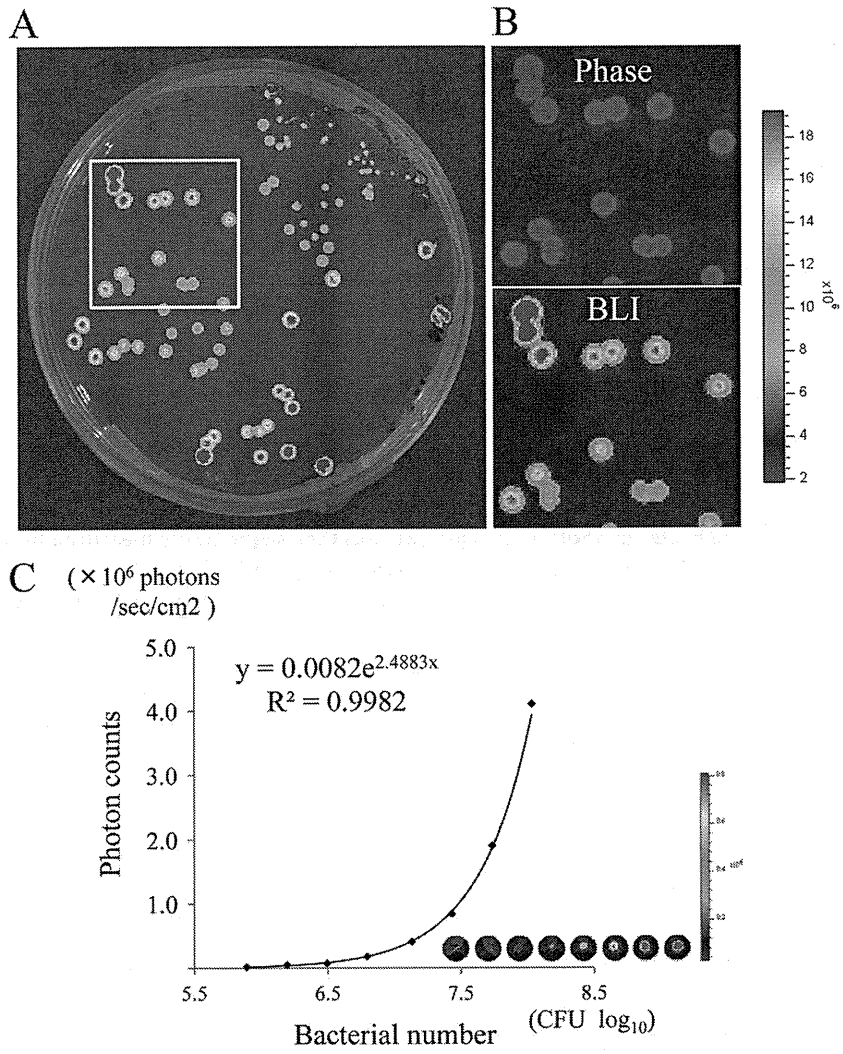

FIG 1 Correlation between bacterial number and bacterial photon intensity *in vitro*. Photon emission of the bacterial bioluminescent signals of *S. aureus* strain Xen-29 was captured as false-color photon count images and quantified by a BLI system. To examine the sensitivity of the BLI, a CCD-based macroscopic detector was used to quantify the bacterial PI (photons/s/cm^2/sr) at various bacterial numbers (7.8×10^5 to 1.0×10^8 CFU per well). Bioluminescent signals were detected from colonies of bioluminescent *S. aureus in vitro* (A and B), and there was a significant correlation between the number of bacterial CFU and the bacterial PI *in vitro* ($R^2 = 0.998$) (C).

Japan) were used in this study. The mice were maintained in our animal facility under specific-pathogen-free conditions. The mice were anesthetized with an intraperitoneal injection of 50 mg of pentobarbital/kg of body weight, and the skin on the left knee was shaved and sterilized with povidone iodine. A skin incision was made over the left knee, and the distal femur was exposed through a lateral parapatellar arthrotomy with medial displacement of the quadriceps-patellar complex. The distal end of the femur was perforated using a high-speed drill with a 0.5-mm sharp steel burr (Fine Science Tools Inc., Foster city, CA). Then, a channel was created using a 23-gauge (external diameter, 0.6 mm) needle, through which the bioluminescent strain of *S. aureus* (1.0×10^8 CFU) in 1 μl of medium was inoculated into the medullary cavity of the femur using a Hamilton syringe. Phosphate-buffered saline (PBS) was administered to the control group using the same technique. The burr hole was closed with bone wax, the dislocated patella was reduced, and the muscle and skin openings were closed by sutures. The animals were placed on a heating pad and carefully monitored until recovery. The observation of spontaneous forelimb movement and the drinking of water were the criteria used to determine that the animals had recovered from the anesthesia.

To measure and analyze the bacterial bioluminescent signal by BLI, the mice were anesthetized via inhalation of aerosolized isoflurane mixed with oxygen. The animals were laid on their backs and imaged for 5 min. All experiments were approved by the Animal Care and Use Committee of Keio University.

BLI. A Caliper LS-Ivis Lumina cooled CCD optical macroscopic imaging system (Summit Pharmaceuticals International Co., Tokyo, Japan) (30) was used for the BLI. Photon emissions of the bacterial bioluminescent signal were captured, converted to false-color photon count images, and quantified with Living Image version 3.0 software (Caliper LS Co., Hopkinton, MA). The bacterial photon intensity (PI) was expressed as photon flux in units of photons/s/cm^2/sr. To quantify the bacterial luminescence, regions of interest (ROIs) were defined in the bacterial plates or inoculated areas and examined. To evaluate the luminescence expression of the bacteria, we first examined whether various numbers of bacteria correlated with the bacterial PI *in vitro* and *in vivo*. To analyze the time course of the infection *in vivo*, the bacterial PI in an ROI was sequentially measured on days 1, 3, 7, 14, and 21 after the operation.

Serological evaluation. Blood samples were collected from the infected and the control mouse groups by retro-orbital bleeding before surgery (day 0) and on days 0.5 (12 h), 1, 3, 7, 14, and 21 after the operation.

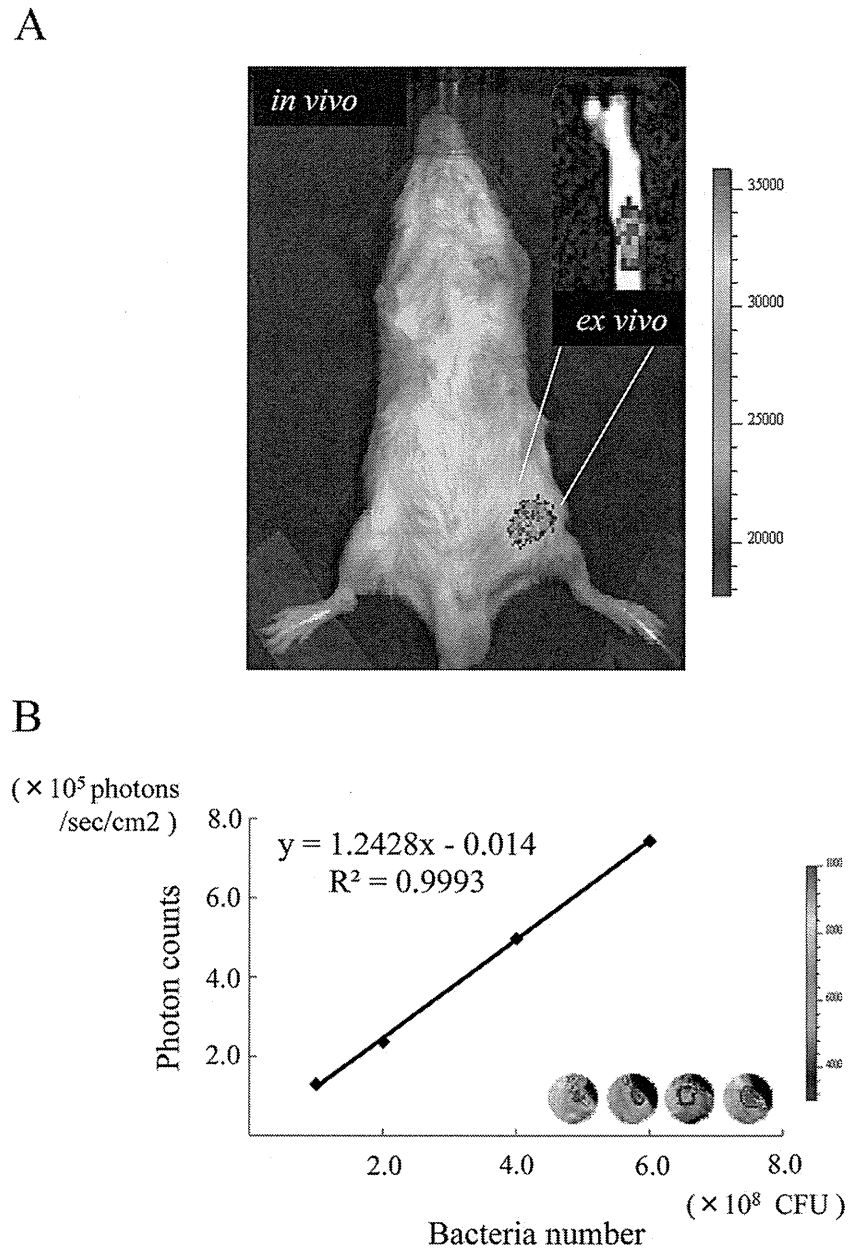

FIG 2 Correlation of bacterial number and bacterial photon intensity *in vivo*. (A) During *ex vivo* imaging, the bacterial bioluminescent signal was detected only in the medullary cavity of the femur and not in the surrounding tissue. (B) Different amounts of bacteria (1.0×10^8 to 6.0×10^8 CFU per inoculation) were inoculated into the femurs, and the bioluminescence in the ROIs was monitored by the BLI system. Significant correlation was observed between the inoculated bacterial number and the bacterial PI *in vivo* ($R^2 = 0.999$).

To measure inflammatory cytokines and chemokines, the sera of both groups were serially diluted, and interleukin-6 (IL-6), IL-1β, C-reactive protein (CRP), and monocyte chemotactic protein 1 (MCP-1) were measured by using enzyme-linked immunosorbent assay (ELISA) kits (R&D Systems, Minneapolis, MN; Kamiya Biomedical Co., Seattle, WA). Detection was carried out according to the manufacturers' instructions.

Flow cytometry. Peripheral blood samples from the infected and the control mice were subjected to double immunofluorescence staining and analyzed by flow cytometry on days 1, 3, 7, 14, and 21 after the operation. Fluorescein isothiocyanate (FITC)–anti-CD11b (clone M1/70) and phycoerythrin (PE)–anti-Ly-6C (Gr-1) (clone RB6-8C5) antibodies (Abs) were purchased from BD Biosciences (San Diego, CA). To block the nonspecific binding of Abs to Fc receptors, the isolated cells were incubated with an anti-CD16/32 monoclonal Ab (MAb) (clone 2.4G2; 1:250) at 4°C for 20 min. The cells were then stained with a mixture of fluorochrome-labeled MAbs at 4°C for 20 min, washed, and incubated with 7-aminoactinomycin D (1:500; BD Biosciences, San Diego, CA) at 4°C for 5 min. Flow cytometry was performed on a FACSCalibur (BD Biosciences, San Diego, CA), and the data were analyzed with FlowJo software (Tree Star, Ashland, OR). Murine granulocytes were defined as SSC^{high} (1× side scatter is 0.15 M NaCl plus 0.015 M sodium citrate) $CD11b^+$ cells (29). These cells also expressed Gr-1 (not shown).

Histological analysis. Femur specimens were collected and analyzed histologically on days 3, 7, 21, and 28 after the operation in both groups. The mice were sacrificed, and the femurs were removed and separated from the soft tissues. The samples were fixed in 4% paraformaldehyde and

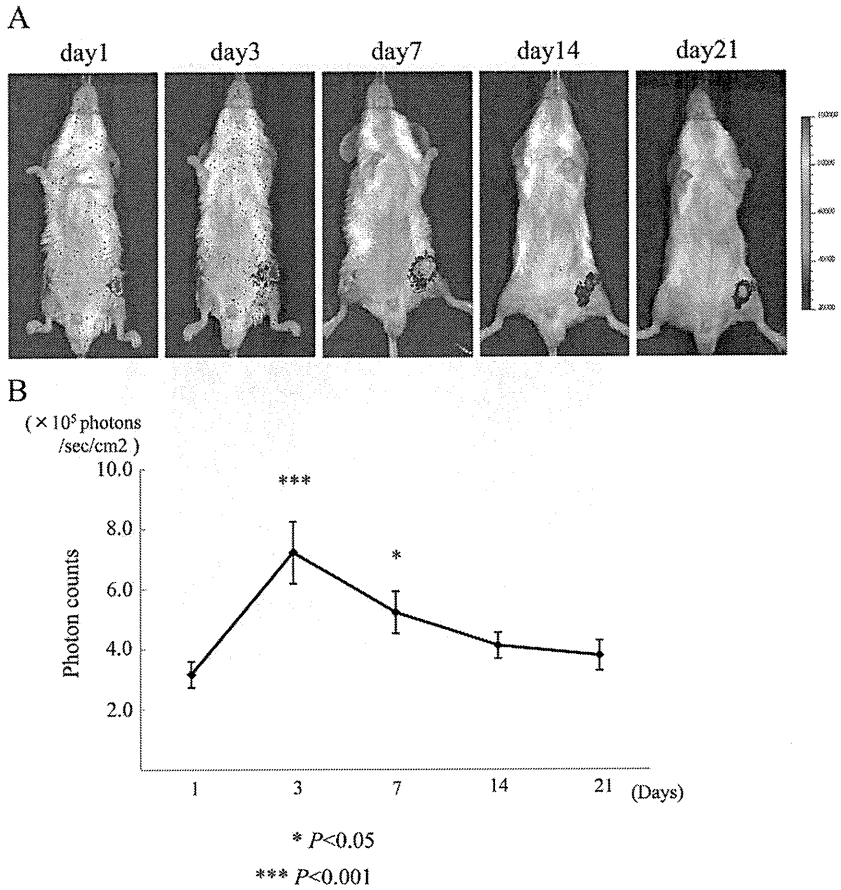

FIG 3 Time course changes of bacterial photon intensity in the mouse osteomyelitis model. *S. aureus* strain Xen29 (1.0×10^8 CFU) in 1 μl of medium was inoculated into the medullary cavity of the femur. The bacterial PI from an ROI was then sequentially measured on days 1, 3, 7, 14, and 21 after surgery ($n = 6$ for each time point). The mean bacterial PI in the infected group peaked on day 3 ($7.2 \times 10^5 \pm 1.0 \times 10^5$ PI) and remained at a high level until approximately day 7 ($5.2 \times 10^5 \pm 0.7 \times 10^5$ PI). Shown are means ± standard errors of the mean (SEM).

demineralized with EDTA. The samples were then embedded in paraffin, cut into 5-μm-thick sections, and stained with hematoxylin and eosin or Gram stain.

Statistical analysis. Correlations between the bacterial CFU and the bacterial PI *in vitro* and *in vivo* were analyzed by linear regression. Changes in the bacterial PI in the infected group were analyzed with Student's *t* test. One-way analysis of variance (ANOVA) and the Fisher *post hoc* test were used to compare the levels of IL-6, IL-1β, CRP, and MCP-1 in serum and the proportion of granulocytes in the peripheral blood between the two groups. Correlation between the bacterial PI and the serum CRP levels was determined using Pearson's correlation coefficient. SPSS II software (IBM-SPSS, Tokyo, Japan) was used, and a *P* value of less than 0.05 was considered significant in all the statistical analyses.

RESULTS

Correlation between bacterial number and bacterial photon intensity *in vitro*. A bioluminescent signal that was sufficient to yield a significant value over background was detected by the BLI system from a single colony of the bioluminescent strain *S. aureus* Xen-29 cultured in Luria Bertani medium (Fig. 1A and B). To examine the sensitivity of the BLI, we used a CCD-based macroscopic detector to measure the PI of bacterial samples with 7.8×10^5 to 1.0×10^8 CFU/well. A minimum of 7.8×10^5 CFU of bacteria was sufficient to produce a detectable signal above the background noise. This quantitative bioluminescence analysis revealed that there was a significant correlation between the number of bacterial CFU and the bacterial PI *in vitro* ($R^2 = 0.998$) (Fig. 1C). To confirm that only live *S. aureus* naturally emitted the luminescent signals, colonies of *S. aureus* bacteria fixed with 4% paraformaldehyde were visualized with the BLI system. No signal was detected from the fixed bacteria (data not shown).

Correlation between bacterial number and bacterial photon intensity *in vivo*. To visualize the infected site *ex vivo*, immediately after the intrafemural inoculation of *S. aureus*, the infected femur was removed and separated from the soft tissues, and the exposed femur was monitored by the BLI system. The bacterial bioluminescent signals were detected only in the medullary cavity of the femur and not in the surrounding tissue (Fig. 2A). To examine whether the number of inoculated bacteria correlated with the bacterial PI *in vivo*, we performed inoculations with different numbers of bacteria (1.0×10^8 to 6.0×10^8 CFU per inoculation) and measured the bacterial PI. As shown in Fig. 2B, there was a significant correlation between the number of inoculated bacteria and the bacterial PI ($R^2 = 0.999$).

Time course of bacterial photon intensity in the mouse OM model. Immediately after the inoculation of *S. aureus* (1.0×10^8 CFU) in 1 μl of medium into the femur, stable luminescent signals were observed in all the animals. Sequential analyses of the bacte-

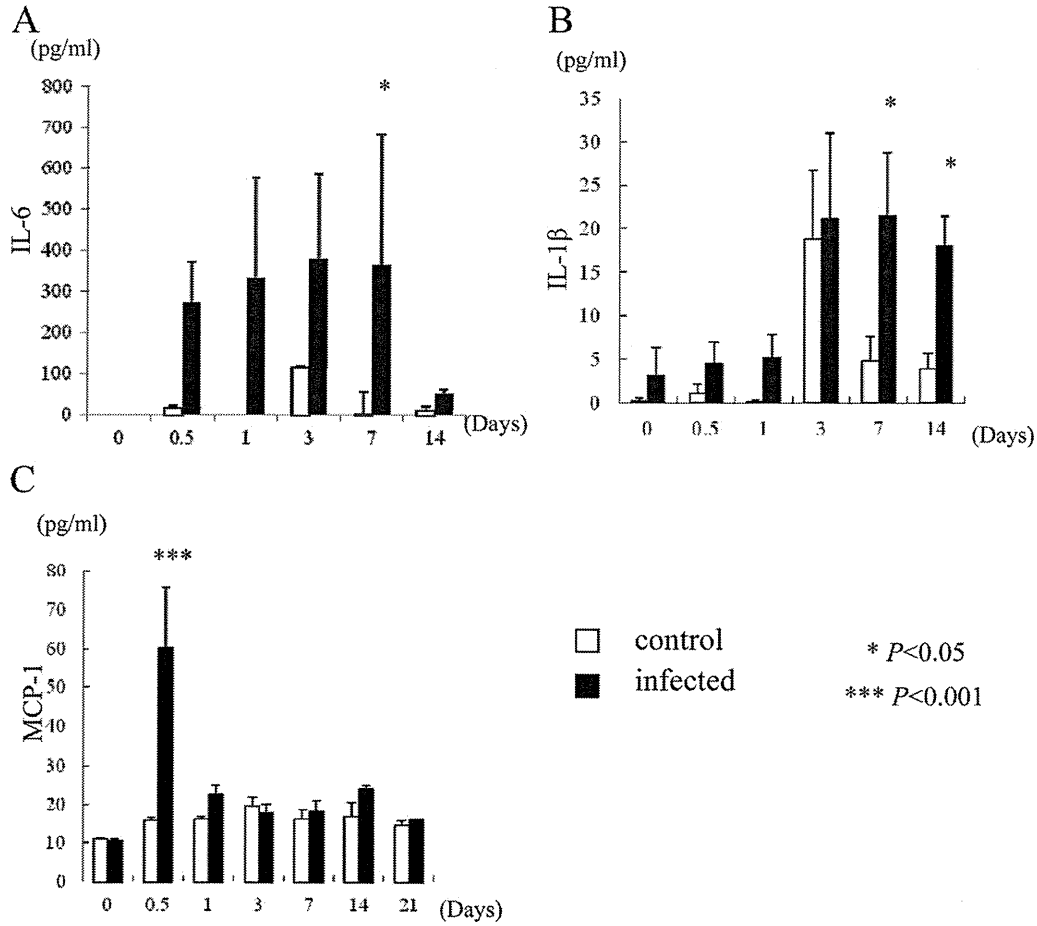

FIG 4 Serological evaluation of control and infected groups. Blood samples from the site of retro-orbital bleeding were collected from the mice before surgery (day 0) and on days 0.5 (12 h), 1, 3, 7, 14, and 21 after the operation in the infected and the control groups ($n = 3$ each). The serum IL-6 (A), IL-1β (B), and MCP-1 (C) levels were measured with ELISA kits. Shown are means ± SEM.

rial luminescence revealed that the mean bacterial PI in the infected group peaked on day 3 ($7.2 \times 10^5 \pm 1.0 \times 10^5$ PI) and remained at a high level until approximately day 7 ($5.2 \times 10^5 \pm 0.7 \times 10^5$ PI) (Fig. 3). Notably, the strong bacterial bioluminescent signal was detected only at the injection site of the femur, and the surrounding tissue was free of infection for 3 months after surgery (data not shown). These observations indicated that this novel mouse model is reproducible and suitable for evaluating the pathophysiology of both acute and chronic osteomyelitis.

Serological evaluation. During the early phase of infection, the mean serum IL-6 and IL-1β levels in the infected group were elevated. The serum IL-6 level was significantly higher in the infected group than in the control group on day 7 ($P < 0.05$) (Fig. 4A). The mean serum level of IL-1β in the infected group was significantly higher on days 7 and 14 ($P < 0.05$) (Fig. 4B). On day 0.5 (12 h), the mean level of MCP-1 was significantly higher in the infected group than in the control group ($P < 0.001$) (Fig. 4C). The mean serum CRP level increased quickly in both groups and remained at 20 ng/ml for 3 days, after which the level remained significantly higher in the infected group on days 7, 14, and 21 ($P < 0.001$) (Fig. 5A). There appeared to be a direct correlation between the bacterial PI and the serum CRP level in the samples obtained on days 14 and 21 ($n = 3$ each), the chronic phase of infection ($r = 0.85$; $P < 0.05$) (Fig. 5B).

Flow cytometry. Flow cytometric analyses using anti-CD11b and anti-Gr1 MAbs showed the presence of granulocytes in the peripheral blood in both groups (Fig. 6). The proportion of SSC^{high} $CD11b^+$ granulocytes in the peripheral blood was significantly higher in the infected group than in the control group on days 7, 14, and 21 ($n = 4$ each) (Fig. 6C).

Histological analysis. On day 21, the femur bone marrow from the sham-treated mice contained the normal cellular components of bone marrow: megakaryocytes, erythroid cells, and myeloid cells. In contrast, on day 3, bacterial colonies were detected in the medullary cavity of the infected mouse femur, along with a marked infiltration of neutrophils. The bacterial colonies were Gram positive. New bone formation started beneath the periosteum on day 7. By day 21, new bone formation and trabecular bone resorption by osteoclasts were present. Manifestations of chronic osteomyelitis, such as sequestrum, new bone formation, and fibrosis, were prominent on day 28 (Fig. 7).

DISCUSSION

Osteomyelitis is a serious infectious disease characterized by progressive bone destruction and formation (1, 19). In most cases, chronic osteomyelitis requires the administration of antibiotic drugs for prolonged periods and sometimes surgical procedures. Recently, the incidence of serious nosocomial infection due to

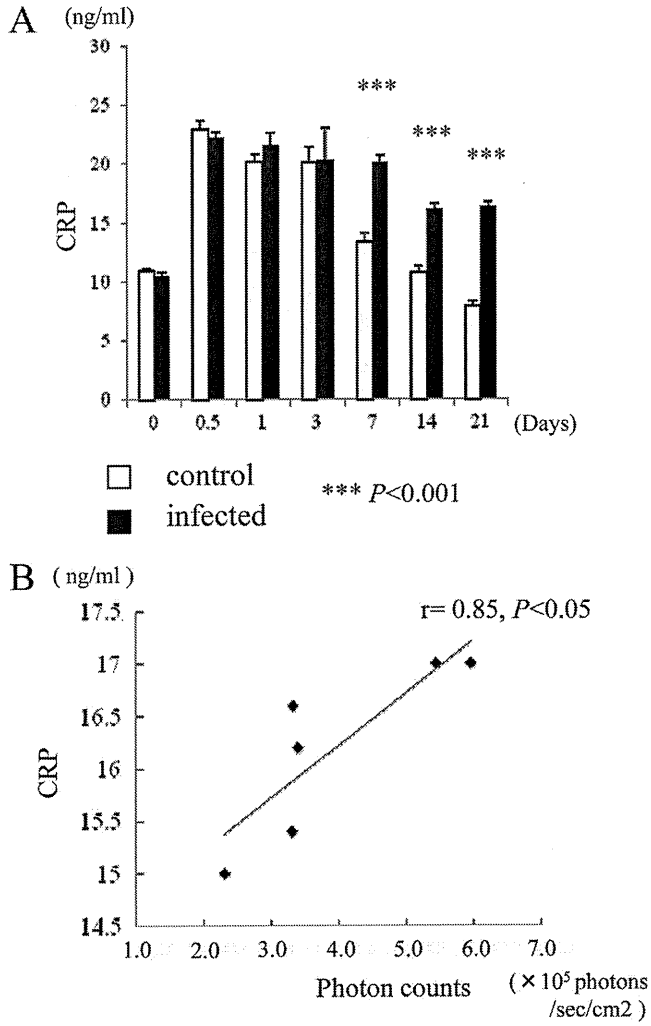

FIG 5 Serum CRP levels. (A) Correlations of bacterial photon intensity and the serum CRP level. The serum CRP levels in the infected and control groups were also measured with ELISA kits (n = 3 each). Shown are means ± SEM. (B) The bacterial CFU and bacterial PI are correlated. The serum CRP concentration was examined in the same samples from mice on days 14 (n = 3) and 21 (n = 3). A direct correlation between the bacterial PI and the serum CRP concentration was observed on both days (r = 0.85; $P < 0.05$).

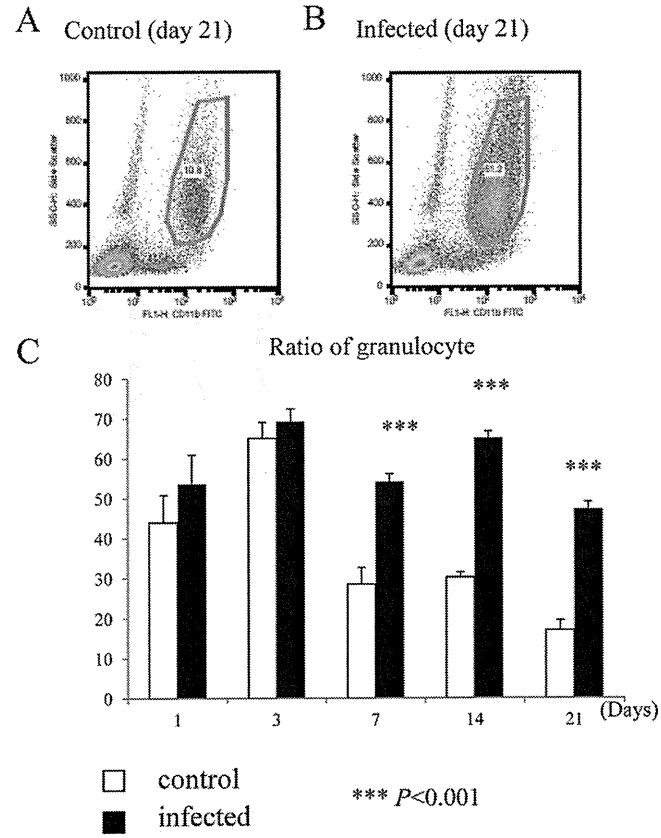

FIG 6 Proportion of granulocytes in the peripheral blood. (A and B) Peripheral blood samples were analyzed by flow cytometry on days 0.5 (12 h), 1, 3, 7, 14, and 21 after the operation in the infected and the control groups. Flow cytometric analyses of SSC^{high} $CD11b^{+}$ granulocytes in the peripheral blood of the control (A) and infected (B) mice on day 21 are shown. (C) The proportions of SSC^{high} $CD11b^{+}$ granulocytes in the peripheral blood on days 7, 14, and 21 were significantly higher in the infected group than in the control group (n = 4 each). Shown are means and SEM.

multiple-drug-resistant strains of bacteria has risen. Thus, the treatment of osteomyelitis has become more difficult (32, 44). Additional sources of rapidly spreading infections include orthopedic implants, such as those used in fracture fixations, arthroplasty, and spinal surgery (8, 39). A number of infection models have been created to study the diagnosis and treatment of osteomyelitis. For example, some investigators have attempted to implant staphylococci intravenously or directly into the bone. Although they successfully produced bone infections, these lesions were not progressive enough to simulate human osteomyelitis (31). Scheman et al. (35) established a reproducible model of chronic osteomyelitis in rabbits by injecting sodium morrhuate and *S. aureus* directly into the tibial metaphysis. Experimental models using small animals, such as rats and mice, allow easy handling and are cost-effective; in particular, mice are especially useful for understanding the pathophysiology of osteomyelitis because various genetically modified mice are commercially available. In recent papers, tibia infection mouse models have been used to evaluate implant-associated osteomyelitis (20, 36). However, because the mouse has tibial curvature with a short medullary cavity and scant surrounding soft tissue, the preparation of this model is technically difficult and often associated with incidental tibial fractures or leakage of the inoculated bacteria. In comparison, our novel osteomyelitis model using the mouse femur is easy and reproducible, because the medullary cavity is straight, with a long, thick cortex and adequate soft tissues surrounding the bone.

In previous animal models of osteomyelitis, the animals had to be sacrificed to quantify the bacterial burden and to assess the extent of infection and inflammation (7). Experiments using such models are very time-consuming, and there is an increased possibility of technical errors during sampling. Furthermore, since the animals have to be sacrificed at certain time points, it is impossible to monitor the same animal throughout the course of the infection. In contrast, recently developed BLI techniques enable us to monitor sequential gene expression patterns and the viabilities of the implanted cells or inoculated bacteria throughout the course of diseases without sacrificing the animal. Moreover, appropriately prepared animals can be selected at the outset of the experi-

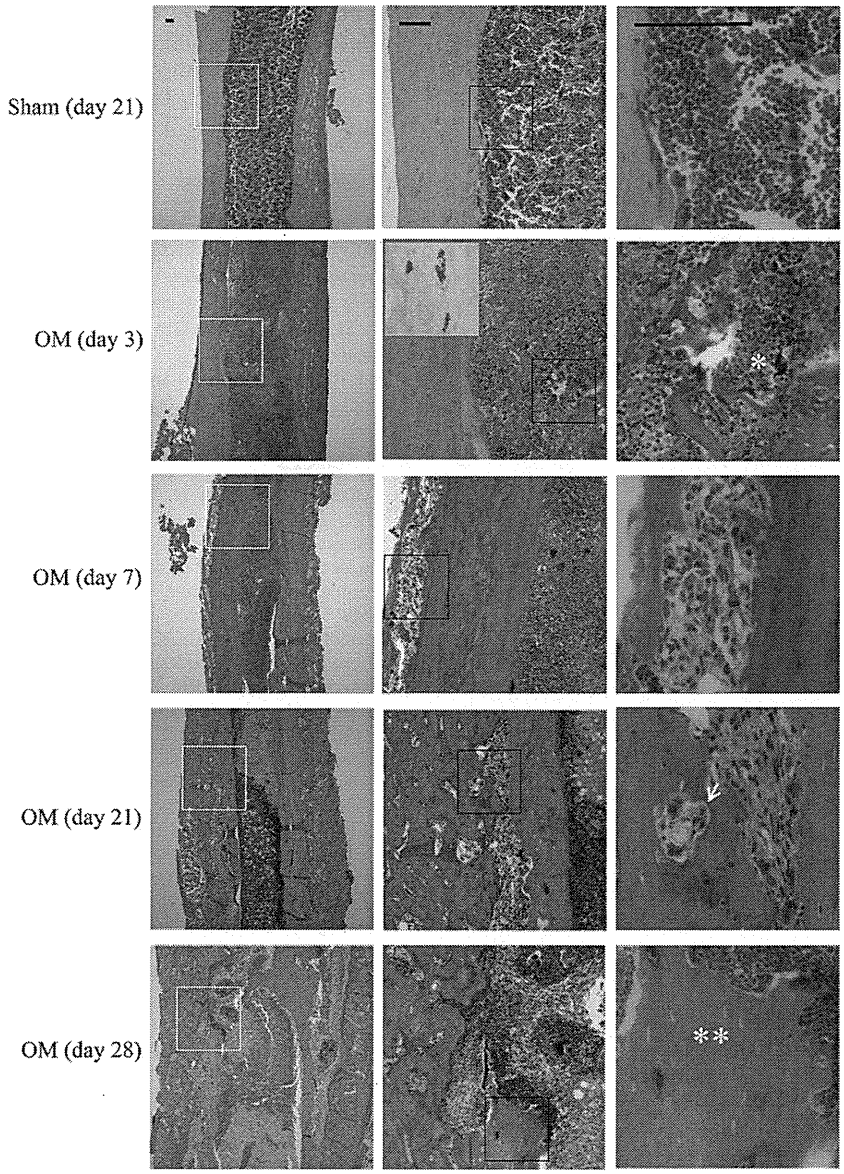

FIG 7 Changes over time in the histology of femurs from infected and control mice. Shown are hematoxylin and eosin staining of longitudinal sections of the uninfected and infected femurs on days 3, 7, 21, and 28 after bacterial inoculation. The middle and right images show higher-power views of the white-boxed areas of the left images and black-boxed areas of the middle images, respectively. The inset of the infected femur (day 3) indicates Gram-stain-positive bacteria. *, necrotic area with bacterial colonies; arrows, osteoclasts; **, sequestrum. Both acute and chronic manifestations of osteomyelitis were observed in this model. Bars = 100 μm.

ment, because the bacterial bioluminescence is visible and can be quantified immediately, thus enabling the accurate evaluation of a treatment and avoiding unnecessary follow-ups. Several studies have shown the advantages of *in vivo* BLI for the real-time monitoring of bacterial infections and their treatment (2, 5, 11, 14, 20, 24, 34, 42). In our mouse osteomyelitis model, sequential analysis of the bacterial luminescence revealed that the bacterial signal peaked on day 3 after the inoculation and then plateaued until day 7 and could be visualized for over 3 months. This time course is similar to that in the previous osteomyelitis models (2, 20), in which the innate immune system contributes to inhibiting the growth of the bacteria at the early phase (20). Recently, Bernthal et al. (2) established a mouse model of implant-associated infection as a preclinical screening tool. However, a limitation of their model is the use of the SH1000 *S. aureus* bioluminescent strain, in which the *lux* genes are contained in a plasmid. The plasmid is stable for only the first 3 days of broth culture, so it is difficult to estimate bacterial numbers by the bioluminescent signals of the strain after 3 days. Thus, their model represents only acute, not chronic, infection. In our model, the *lux* genes were inserted into the *S. aureus* chromosome and the bioluminescent signals were maintained for a longer period. In addition, leakage of the inoculated bacteria to surrounding tissues is often observed in implant-associated osteomyelitis and joint infection models and can be a major cause of skin ulcers. Such models are poorly reproducible, with short, unstable emission of the bacterial luminescence. In